International Journal of Pharmaceutics 434 (2012) 9–19

Contents lists available at SciVerse ScienceDirect

International Journal of Pharmaceutics

journal homepage: www.elsevier.com/locate/ijpharm

Pharmaceutical Nanotechnology

Toward a siRNA-containing nanoparticle targeted to breast cancer cells and the tumor microenvironment

Lígia C. Gomes-da-Silva[a,b], Adriana O. Santos[a,b], Luís M. Bimbo[a,b], Vera Moura[a,b], José S. Ramalho[c], Maria C. Pedroso de Lima[a,d], Sérgio Simões[a,b], João N. Moreira[a,b,*]

[a] CNC - Center for Neurosciences and Cell Biology, University of Coimbra, Portugal
[b] FFUC - Faculty of Pharmacy, University of Coimbra, Portugal
[c] Laboratory of Cellular and Molecular Biology, Faculty of Medical Sciences, New University of Lisbon, Portugal
[d] Department of Life Sciences, Faculty of Sciences and Technology, University of Coimbra, Portugal

ARTICLE INFO

Article history:
Received 26 February 2012
Received in revised form 6 May 2012
Accepted 11 May 2012
Available online 19 May 2012

Keywords:
Dual-targeted delivery
Ligand-mediated targeting
Stable nucleic acid lipid particles (SNALP)
siRNA
Breast cancer

ABSTRACT

The present work aimed at designing a lipid-based nanocarrier for siRNA delivery toward two cell sub-populations within breast tumors, the cancer and the endothelial cells from angiogenic tumor blood vessels. To achieve such goal, the F3 peptide, which is specifically internalized by nucleolin overexpressed on both those sub-populations, was used as a targeting moiety.

The developed F3-targeted stable nucleic acid lipid particles presented adequate features for systemic administration. In addition, the attachment of the F3 peptide onto the liposomal surface enabled an internalization by both cancer and endothelial cells from angiogenic blood vessels that was significantly higher than the one observed with non-cancer cells. Sequence-specific downregulation of enhanced green fluorescent protein (eGFP) in *eGFP*-overexpressing human cancer cell lines, both at the protein and mRNA levels, was further observed upon delivery of anti-*eGFP* siRNA by F3-targeted liposomes, in contrast with the non-targeted counterpart. This effect was highly dependent on the content of poly(ethylene glycol) (PEG), as evidenced by the co-localization studies between the siRNA and the lysosomes.

Overall, the present work represents an important contribution toward a nanoparticle with multi-targeting capabilities in breast cancer, both at the cellular and molecular level.

1. Introduction

Cancer is still a severe public health problem being one of the most deadly diseases in the western world (Jemal et al., 2011). The limited effectiveness of conventional treatment strategies has generated considerable interest on the development of novel anticancer agents, with improved molecular target specificity. In this context, small-interfering RNA (siRNA), 21–23 nucleotides long double-stranded RNA that inhibit the expression of a target gene through specific cleavage of perfectly complementary mRNA (Elbashir et al., 2001a,b; Fire et al., 1998), may constitute a novel class of pharmaceutical drugs, as they can potently and specifically inhibit the expression of any intracellular protein involved in tumor initiation and/or progression. However, the translation of these molecules from the bench to the clinic has been hindered by their limited cellular uptake, low biological stability and unfavorable pharmacokinetics (Castanotto and Rossi, 2009; Moreira et al., 2008).

In order to overcome the mentioned limitations, different types of poly(ethylene glycol) (PEG)-grafted liposomes have been developed such as, stabilized antisense lipid particles (SALP) (Maurer et al., 2001; Semple et al., 2001), or the related stabilized nucleic acid lipid particles (SNALP) encapsulating siRNA (Akinc et al., 2010; Geisbert et al., 2006; Judge et al., 2009; Morrissey et al., 2005; Zimmermann et al., 2006). The PEG-derivatized lipid in the liposomal formulation forms a hydrophilic shell around the liposomes that, upon intravenous administration, decreases the rate and the extent of electrostatic and hydrophobic interactions between the surface of liposomes and the blood components that mediate liposomal blood clearance (Allen and Hansen, 1991; Allen et al., 1991; Papahadjopoulos et al., 1991). In addition, those systems are also characterized by high nucleic acid encapsulation, nucleic acid protection from serum nucleases, a small average size, and a net charge close to neutrality, thus making them adequate for intravenous administration. Although pegylated systems can exhibit passive accumulation into a tumor due to their large fenestrated endothelium (enhanced permeability and retention, EPR, effect (Fang et al., 2011; Iyer et al., 2006)), large improvements can be achieved

* Corresponding author at: Center for Neurosciences and Cell Biology, University of Coimbra, Largo Marquês de Pombal, 3004-517 Coimbra, Portugal.
Tel.: +351 916885272.
E-mail address: jmoreira@ff.uc.pt (J.N. Moreira).

0378-5173/$ – see front matter © 2012 Elsevier B.V. All rights reserved.
http://dx.doi.org/10.1016/j.ijpharm.2012.05.018

through the covalent attachment of internalizing targeting ligands, which will interact specifically with receptors overexpressed on the surface of target cells (Moreira et al., 2008; Torchilin, 2010).

However, the design of novel targeted anticancer strategies must take into account that the aggressiveness of a tumor does not rely only on the cancer cell, but rather on the cross-talk between cancer cells and other cells from the tumor microenvironment such as, the endothelial cells (Hanahan and Weinberg, 2011). Thus, targeting angiogenesis, in addition to cancer cells, can significantly improve clinical efficacy, as tumor growth and metastases formation are angiogenesis-dependent (Abdollahi and Folkman, 2010). Furthermore, vascular targeting carries some additional advantages since endothelial cells are more accessible (than cancer cells) to the therapeutic agent injected in the vascular compartment, and are less prone to acquire drug resistance. In addition, treatment selectivity can be achieved, as, besides tumors, the formation of new blood vessels is restricted to a few physiological processes such as wound healing, ovulation and pregnancy (Abdollahi and Folkman, 2010).

The F3 peptide, which is specifically internalized by nucleolin, a receptor overexpressed on the surface of cancer and endothelial cells of tumor blood vessels, offers the possibility to develop dual-targeting strategies for nucleic acid delivery (Christian et al., 2003; Porkka et al., 2002).

Therefore, the main aim of this work was to design F3-targeted SNALP for the encapsulation, protection and effective intracellular delivery of siRNA to two cell populations within a tumor: the cancer cells and the endothelial cells from angiogenic blood vessels.

2. Materials and methods

2.1. Materials

Lipids, 1,2-dioleoyl-3-dimethylammonium-propane (DODAP), 1,2-distearoyl-*sn*-glycero-3-phosphocholine (DSPC), N-palmitoyl-sphingosine-1-[succinyl(methoxypolyethylene glycol)$_{2000}$] (CerC_{16}PEG$_{2000}$), 1,2-distearoyl-*sn*-glycero-3-phospatidylethanolamine-N-[maleimide (polyethylene glycol)$_{2000}$] ammonium salt (DSPE-PEG-MAL) and L-α-phosphoethanolamine-N-(lissamine rhodamine B sulfonyl) (Rho-PE) were purchased from Avanti Polar Lipids (USA). The lipid, cholesterol (CHOL), was obtained from Sigma (Germany).

The anti-e*GFP* siRNA (5′GAA CUU CAG GGU CAG CUU GCdTdT-3′), the control siRNA (5′-GUC UCA AGU UUU CGG GAA GdTdT-3′) and the FITC-labeled anti-e*GFP* siRNA were purchased from Dharmacon (USA).

The 31 aminoacid F3 peptide (KDEPQRRSARLSAKPAPPKPEPKPKKAPAKK) and the non-specific (NS) peptide were purchased from Genecust (Luxembourg) (Porkka et al., 2002).

2.2. Cell lines

The human breast cancer cell lines, MDA-MB-435S and MDA-MB-231, and the human fibroblasts, BJ, were from American Type Culture Collection (ATCC). The human microvascular endothelial cell line, HMEC-1, was a generous gift from the Center for Disease Control and Prevention (USA).

MDA-MB-435S and MDA-MB-231 were cultured in RPMI 1640 medium (Sigma, Germany) and human fibroblasts cells, BJ, were cultured in DMEM medium (Sigma, Germany). Both media were supplemented with 10% (v/v) heat-inactivated fetal bovine serum (Invitrogen, USA), and 100 U/ml penicillin, 100 μg/ml streptomycin (Invitrogen, USA). HMEC-1 cells were cultured in RPMI 1640 supplemented with 10 ng/ml of mouse epidermal growth factor (mEGF) (Sigma, Germany) and 1 μg/ml hydrocortisone (Sigma, Germany). Cells were maintained in exponential growth phase, at 37 °C, in a 90% humidified atmosphere containing 5% CO_2.

2.3. Preparation of sterically stabilized liposomes

Preparation of stabilized nucleic acid lipid particles (SNALP) was adapted from Semple et al. (Maurer et al., 2001; Semple et al., 2001). A lipid mixture of DODAP:DSPC:CHOL:CerC_{16}-PEG$_{2000}$ (30:23:45:2, 30:21:45:4 or 30:15:45:8, % molar ratio relative to total lipid, 13 μmol) in absolute ethanol and 0.046 μmol of anti-e*GFP* siRNA or of a non-specific siRNA in 20 mM citrate buffer, pH 4, were heated at 65 °C. For cellular association and internalization studies, nanoparticles were double-labeled with anti-e*GFP* FITC-labeled siRNA and 1 mol% of Rho-PE.

The lipid mixture was added, slowly and under strong agitation, to the siRNA solution. The resulting particles were then extruded 21 times through polycarbonate membranes of 100 nm pore diameter, using a LiposoFast basic extruder (Avestin, Canada). Removal of ethanol and non-encapsulated siRNA was carried out upon running extruded nanoparticles through a Sepharose CL-4B column equilibrated with HEPES buffered saline (HBS) (20 mM HEPES, 145 mM NaCl), pH 7.4.

2.4. Preparation of targeted liposomes

Targeted liposomes were prepared by the post-insertion method (Moreira et al., 2002; Santos et al., 2010). Briefly, F3 and NS peptides were first thiolated upon reaction with 2-iminothiolane in HBS, pH 8, during 1 h at room temperature, in an inert N_2 atmosphere. They were then coupled to DSPE-PEG-MAL micelles, prepared in MES buffered saline (MBS) (20 mM MES, 20 mM HEPES), pH 6.5. Insertion of DSPE-PEG-MAL-F3 or DSPE-PEG-MAL-NS conjugates onto the preformed sterically stabilized liposomes previously prepared, took place upon incubation of the corresponding micelles with the latter at 50 °C for 1 h. For the non-targeted lipid particles, post-insertion was performed only with plain DSPE-PEG-MAL micelles. Neutralization of non-reacted maleimide groups was performed upon incubation with 2-mercaptoethanol at a maleimide/2-mercaptoethanol molar ratio of 1:5. Finally, liposomes were run through a Sepharose CL-4B column equilibrated with HBS, pH 7.4.

2.5. Characterization of the liposomes

The final total lipid concentration was inferred from the cholesterol concentration, determined with the Infinity® liquid stable reagent (Thermo Scientific, USA). The quantification of the siRNA that was encapsulated into the liposomes was determined with the Quanti-iT™ Ribogreen reagent (Invitrogen, USA), in the presence of octaethylene glycol monododecyl ether ($C_{12}E_8$) detergent (Sigma, Germany). The encapsulation efficiency was calculated from the formula $[(\text{siRNA/total lipid})_{\text{final molar ratio}}/(\text{siRNA/total lipid})_{\text{initial molar ratio}}] \times 100$. In order to assess if the siRNA was fully encapsulated and protected by the lipid nanoparticle, the ability of the probe Quant-iT™ Ribogreen to intercalate with siRNA, in the absence of the detergent $C_{12}E_8$, was evaluated.

The mean diameter of the resulting liposomes was determined by Photon Correlation Spectroscopy, using an N5 submicron particle size analyzer (Beckman Coulter). The zeta potential was assessed using a Particle Size Analyzer 90 Plus (Brookhaven).

To determine the amount of DSPE-PEG-MAL-F3 conjugate that was transferred onto the preformed liposomes, the F3 peptide was quantified using the CBQCA protein quantification Kit (Invitrogen, USA).

2.6. Assessment of cellular association by flow cytometry

Half million of cancer, fibroblast or endothelial cells were seeded in 48-well plate. Twenty four hours later, cells were incubated at 37 or 4 °C, during 1 h, with rhodamine-labeled F3-targeted, NS-targeted or non-targeted liposomes, at 0.2, 0.4 or 0.6 mM of total lipid. Afterwards, cells were washed three times with phosphate buffer saline (PBS), pH 7.4, detached with dissociation buffer and immediately analyzed by flow cytometry using a FACS Calibur flow cytometer (BD, Biosciences). Rhodamine fluorescence was evaluated in the FL2 channel and a total of 20,000 events were collected. Data were analyzed with the Cell Quest Pro software.

2.7. Assessment of cellular internalization by confocal fluorescence microscopy

For the confocal studies, 2.5×10^5 of cancer, fibroblast or endothelial cells were seeded on glass cover slips in 12-well plate and further incubated, at 37 or 4 °C, during 1 h, with 1 μM of FITC-labeled siRNA encapsulated in rhodamine-labeled liposomes (F3-targeted or non-targeted). After washing three times with PBS, cells were fixed with 4% paraformaldehyde, and the nucleus stained with DAPI, washed with PBS, and finally, mounted in mowiol mounting medium. Confocal images were acquired in a Zeiss LSM-510 point scanning confocal microscope (Zeiss, Germany), using a diode (405 nm), an argon (488 nm) and a DPSS excitations lasers for DAPI, FITC and Rhodamine, respectively, and a 63× oil immersion objective. Images were acquired and analyzed using the LSM 510 Meta software. All instrumental parameters pertaining to fluorescence detection and images analyses were held constant to allow sample comparison.

2.8. Evaluation of eGFP levels by flow cytometry

Human cancer cell lines overexpressing eGFP, MDA-MB-435S-eGFP and MDA-MB-231-eGFP, were used to evaluate the potential of the F3-targeted liposomes to downregulate a target protein. EGFP was used as a model target as its downregulation could be easily assessed upon measuring fluorescence by flow cytometry, thus facilitating the assessment of the delivery properties of each one of the formulations to be tested.

In order to evaluate the downregulation of eGFP, 30.000 cells were seeded in 48-well plates. Twenty-four hours later, cells were transfected, at 37 °C during 4 h, with different concentrations of anti-*eGFP* siRNA encapsulated in F3-targeted or non-targeted liposomes, or a non-specific siRNA encapsulated in the former. Afterwards, cell culture medium was replaced with fresh medium and a second transfection was performed 44 h after the beginning of the experiment, with the same formulations and concentrations used in the first transfection. In another set of experiments, single transfections were performed right at the beginning of the experiment, at 37 °C during 4 h. In these experiments, 48 or 96 h after the beginning of the experiment, cells were detached and eGFP levels were evaluated by flow cytometry using a FACS Calibur flow cytometer (BD, Biosciences).

EGFP fluorescence was evaluated in the FL1 channel and a total of 20,000 events were collected. Data were then analyzed with the Cell Quest Pro software. The eGFP fluorescence reduction was expressed in percentage of the ratio: 100 − [(eGFP signal of treated cells/eGFP signal of untreated cells) × 100].

2.9. Intracellular trafficking of siRNA encapsulated in F3-targeted liposomes

In order to investigate whether siRNA encapsulated in the developed F3-targeted liposomes could efficiently escape from endosomes, co-localization studies between the siRNA and the lysosomes were performed in MDA-MB-435S cells.

Cancer cells were seeded on μ-slide 8-well ibitreat plates (Ibidi, Germany). After 24 h, cells were incubated with F3-targeted liposomes encapsulating a FITC-labeled siRNA, during 4 h at 37 °C. Afterwards, lysosomes were stained upon cell incubation with 100 nM LysoTracker Red (Invitrogen, USA) for 2 h, followed by washing three times with PBS. Live cells were then immediately visualized using an argon (488 nm), a DPSS (561 nm) and a helium–neon (633 nm) excitations lasers for FITC, Lysotracker Red and differential interference contrast (DIC), respectively, and a 63× oil immersion objective. Images were acquired and analyzed as previously described.

2.10. Evaluation of eGFP mRNA by quantitative real-time reverse-transcription PCR (qRT-PCR)

In order to confirm that the eGFP reduction observed by flow cytometry was due to an RNA interference mechanism, the levels of *eGFP* mRNA were determined by qRT-PCR, 24 h after the second transfection (72 h after the beginning of the experiment).

Cells were harvested and RNA extracted with RNeasy Mini Kit (Qiagen, Germany) according to the manufacturer's instructions. The Quanti-iT™ Ribogreen reagent was used to quantify the extracted RNA, where 0.5 μg of RNA was reversed transcribed into cDNA in a 20 μl reaction mixture using the SuperSript™ III First Strand Synthesis Supermix (Invitrogen, USA) following the manufacturer's instructions.

Quantitative real-time PCR (q-PCR) was performed using the Iq™SYBR Green Supermix (Bio-Rad, USA). *Beta-2-microglobulin* (*β2M*) was used as the endogenous control (housekeeping gene). The forward primer for *β2M* was 5′-GAGTATGCCTGCCGTGTG-3′ and the reverse primer was 5′-AATCCAAATGCGGCATCT-3′ (Microsynth, Switzerland). For *eGFP*, the QuantiTect™ Primer Assay (Qiagen, Germany) was used.

The optimized qPCR conditions included the activation of HotStartTaq Plus DNA polymerase followed by 40 cycles of two steps: a first step of denaturation (10 s at 95 °C) and a second step of combined annealing/extension (30 s at 60 °C). After the qPCR, a melting curve analysis of the PCR products was performed to confirm their specificity. The threshold cycle (Ct) values were generated by the iQ5 Optical System Software. The level of *eGFP* mRNA was calculated by the Livak method, $2^{-\Delta\Delta Ct} \times 100$, where $\Delta\Delta Ct = (Ct\ eGFP – Ct\ \beta 2M)$ treated − (Ct *eGFP*–Ct *β2M*) untreated. The application of this method relied on the similar PCR efficiencies between the target gene and the housekeeping gene.

2.11. Statistical analysis

The results are presented as the mean ± standard deviation (SD) of at least three independent experiments. One- or two-way ANOVA with Bonferroni's post-test was used to determine statistically significant differences of the means. Statistical differences are presented at probability levels of $p > 0.05$, $p < 0.05$, $p < 0.01$, and $p < 0.001$.

3. Results

3.1. Preparation and physico-chemical characterization of F3-targeted and non-targeted liposomes

The pharmacokinetics and biodistribution of any encapsulated drug, regardless its nature, are highly dependent on the physico-chemical properties of the liposomes, including size, surface charge, level of protection against nucleases and the presence of targeting

Table 1
Physico-chemical characterization of F3-targeted and non-targeted liposomes containing anti-e*GFP* siRNA. Values are the mean ± SD of at least 3 independent experiments.

PEG (mol%)	F3-targeted liposomes			Non-targeted liposomes		
	Size (nm)	Polydispersity index	Encaps. efficiency (%)	Size (nm)	Polidispersity index	Encaps. efficiency (%)
2	254.4 ± 26.55	0.144 ± 0.03	95.72 ± 8.44	130.3 ± 13.32	0.076 ± 0.05	99.77 ± 8.48
4	194.7 ± 16.40	0.149 ± 0.03	95.99 ± 21.15	109.0 ± 10.82	0.145 ± 0.05	90.32 ± 12.42
8	210.2 ± 21.74	0.146 ± 0.06	76.86 ± 16.63	112.1 ± 4.51	0.281 ± 0.05	87.53 ± 18.32

moieties at the surface that are specifically recognized by internalizing receptors overexpressed on the target cells (Li and Huang, 2008).

It is well recognized that PEG plays an important role preventing particle aggregation during the preparation process (Maurer et al., 2001). Therefore the impact of the incorporation of different amounts of $CerC_{16}$-PEG_{2000} (2, 4, and 8 mol% relative to total lipid) on the final size of the liposomes was evaluated. For F3-targeted liposomes, an increase in the amount of the PEG-derivatized lipid, from 2 to 4%, led to a decrease on the mean size of the particles reaching values around 200 nm, while exhibiting a narrow particle distribution as the polydispersity index was in the range of 0.14–0.15 (Table 1). We have also verified that the length of the encapsulated siRNA influenced the liposomal mean size. A difference as small as 1 nt on the siRNA length, has resulted in a reduction of around 50 nm in the mean size of targeted liposomes with 2 mol% of $CerC_{16}$-PEG_{2000} (205.70 ± 18.55 nm).

The attachment of the F3 peptide to the surface of liposomes was performed by the insertion (Ishida et al., 1999; Moreira et al., 2002) of DSPE-PEG-MAL-F3 conjugates onto preformed liposomes, leading to an average amount of 4 nmol of F3 peptide per μmol of total lipid. Importantly, this procedure has not interfered with the loading of the encapsulated nucleic acids since encapsulation efficiencies close to 100% have been observed for both non-targeted and F3-targeted liposomes (Table 1). This high siRNA encapsulation efficiency was certain due to the inclusion in the lipid bilayer of the ionizable lipid DODAP, which is positively charged at low pH. However, after siRNA encapsulation, adjustment of the external pH to neutral pH resulted in nanoparticles close to neutrality, which reduces their ability to interact with serum proteins that mediate an early clearance from the blood stream (Li and Huang, 2008). Non-targeted liposomes were slightly negative (−4.83 ± 1.23 mV) while F3-targeted liposomes (0.37 ± 3.48 mV) exhibit a net surface charge close to neutrality likely due to the presence of the F3 peptide on the surface of the particle, which is rich in lysines and thus positively charged.

Regarding the level of nucleic acid protection in both formulations tested, it was observed that in the absence of the membrane-disrupting detergent $C_{12}E_8$, the probe Quant-iT™ Ribogreen was not able to intercalate with the encapsulated siRNA, translated in levels of protection close to 100%. These results indicated that the nanoparticles were efficiently playing one of their primary roles, which consist in the protection against nuclease-mediated degradation.

3.2. Cellular association studies

At 37 °C, the level of cellular association of F3-targeted liposomes was significantly higher than the one observed for the non-targeted liposomes or liposomes coupled to a non-specific peptide. These results indicated that the presence of the F3 peptide at the liposomal surface brought an important gain, as it mediated an important improvement on the extent of cellular association by breast cancer cells, including the triple negative MDA-MB-231 cells, and the endothelial cells from angiogenic blood vessels, HMEC-1 as well (Marchio et al., 2004).

Upon incubation with 0.4 mM of total lipid, a 12-fold or a 14-fold increase in the rhodamine signal for both MDA-MB-231 and HMEC-1 cells or MDA-MB-435S cell lines, respectively, was observed. Regardless the histological origin of the cells, the cellular uptake was dose-dependent (Fig. 1A).

The interaction of the developed F3-targeted liposomes revealed to be peptide-specific as it was pointed out by the low level of cellular association observed with the liposomes coupled to a non-specific peptide. Moreover, in similar experiments performed with a non-cancer (negative control) cell line, BJ fibroblasts, the previous mentioned differences between F3-targeted and non-targeted liposomes were dissipated, thus indicating that the interaction of the former with the target cells was also tumor cell-specific. This observation is of high relevance as it strongly indicated that the proposed strategy would avoid the internalization by normal tissues, thus reducing its potential toxicity (Fig. 1A).

Incubation of F3-targeted liposomes at 4 °C, a temperature non-permissive for endocytosis, strongly inhibited cellular association when compared to incubations at 37 °C, a condition where both binding and endocytosis take place. These results suggested that an energy-dependent process, most likely receptor-mediated endocytosis, was involved in the uptake of F3-targeted liposomes (Fig. 1B).

In order to confirm the previous results, additional cellular association studies were performed and cells analyzed by confocal microscopy. After 1 h of incubation, F3-targeted liposomes were localized in the cytoplasm of cancer (MDA-MB-435S and MDA-MB-231) and endothelial cells (HMEC-1), as can be observed by the intense red and green fluorescence, from rhodamine (marker of the liposomal membrane) and FITC (labeling the encapsulated nucleic acid), respectively. This pattern was not visible neither in the non-cancer BJ fibroblasts nor when any of the tested cells were incubated with non-targeted liposomes. In addition, when MDA-MB-435S cells were incubated with F3-targeted liposomes, at 4 °C, no significant levels of internalization were observed (Fig. 2). Overall, these findings corroborate the previous results observed by flow cytometry thus, also reinforcing the cell-specific interaction of the developed targeted liposomes.

3.3. Evaluation of eGFP levels

For proof-of-concept on the intracellular delivery capabilities of each one of the tested formulations, MDA-MB-435 and MDA-MB-231 cells overexpressing the *enhanced green fluorescence protein* (*eGFP*) were used, along with a siRNA against *eGFP*.

When cells were transfected twice with anti-*eGFP* siRNA delivered by F3-targeted liposomes incorporating 2 mol% of $CerC_{16}$-PEG_{2000} (Fig. 3A and B), a significant concentration-dependent downregulation of the target protein was observed in both MDA-MB-435S (from 19.9 to 42.7%) and MDA-MB-231 (from 17.9 to 29.9%), upon assessment at 96 h after the beginning of the experiment. These results emphasized the importance of the intracellular delivery of the nucleic acid on its activity, as a total absence of eGFP silencing was registered with the non-targeted counterpart. The difference on the extent of eGPF silencing between these two cell

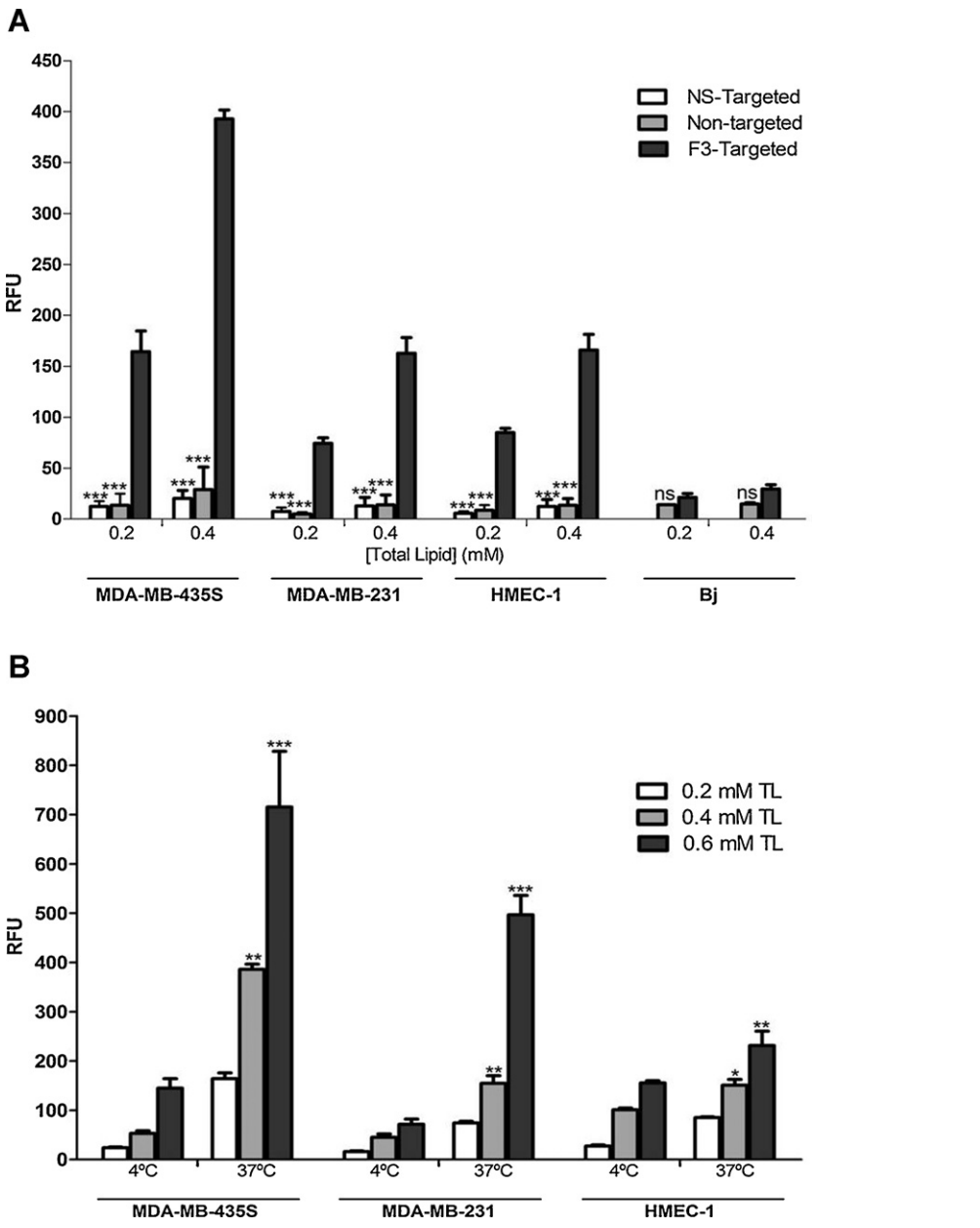

Fig. 1. Extent of cellular association of rhodamine-labeled liposomes with human cancer cell lines, endothelial cells and human fibroblasts analyzed by flow cytometry. MDA-MB-435S and MDA-MB-231 cancer cells, human microvascular endothelial cells (HMEC-1) or human non-cancer BJ fibroblasts (0.5×10^6) were incubated with different concentrations of F3-targeted, targeted by a non-specific (NS) peptide and non-targeted liposomes at (A) 37 °C or (B) 37 °C or 4 °C, during 1 h. After incubation, rhodamine signal was assessed by flow cytometry. Bars are the mean ± SD of 3 independent experiments. Two-way ANOVA analysis of variance with Bonferroni's post-test was used for comparison between the referenced samples and the F3-targeted liposomes. ***$p < 0.001$; **$p < 0.01$; ns: $p > 0.05$.

lines, was likely related with the higher extent of cellular association (and internalization) by the MDA-MB-435S cells (Figs. 1 and 2).

Interestingly, for the same 96 h duration of the experiment no significant differences in the level of eGFP silencing were observed upon performing a single transfection (Fig. 3A and B). Moreover, eGFP signal reduction in MDA-MB-435S-eGFP, 48 h after one single transfection, was lower than the one observed at 96 h (22.3 *versus* 36.1%, at 2 μM siRNA; $p < 0.001$) (Fig. 3A and C). Taken together, these results reflect the ability of the siRNA to be recycled intracellularly over time, thus propagating gene silencing (Hutvagner and Zamore, 2002) and, the low turnover of the target protein as well (Li et al., 1998). The siRNA concentrations required with the proposed F3-targeted strategy were higher than the ones used with regular agents for in *vitro* transfection, like lipofectamine (data not shown), however, they were in accordance with other reports on ligand-mediated targeted (PEGylated) liposomes for the delivery of nucleic acids (Di Paolo et al., 2011; Mendonca et al., 2010).

In order to assess if liposomes with a higher PEG content and therefore more stable from a physical point of view, still maintained the capacity to silence a target protein, MDA-MB-435S-eGFP cells were transfected with anti-*eGFP* siRNA delivered by F3-targeted liposomes incorporating 4 or 8 mol% of $CerC_{16}$-PEG_{2000}. Transfection with 4 mol% of PEG F3-targeted liposomes still enabled downregulation of the target protein (Fig. 3D) but to a lesser extent than the counterpart incorporating 2 mol% PEG (Fig. 3A), whereas the presence of 8 mol% PEG completely prevented gene silencing (data not shown). In MDA-MB-231-eGFP cells a total absence of eGFP silencing was observed even with targeted liposomes

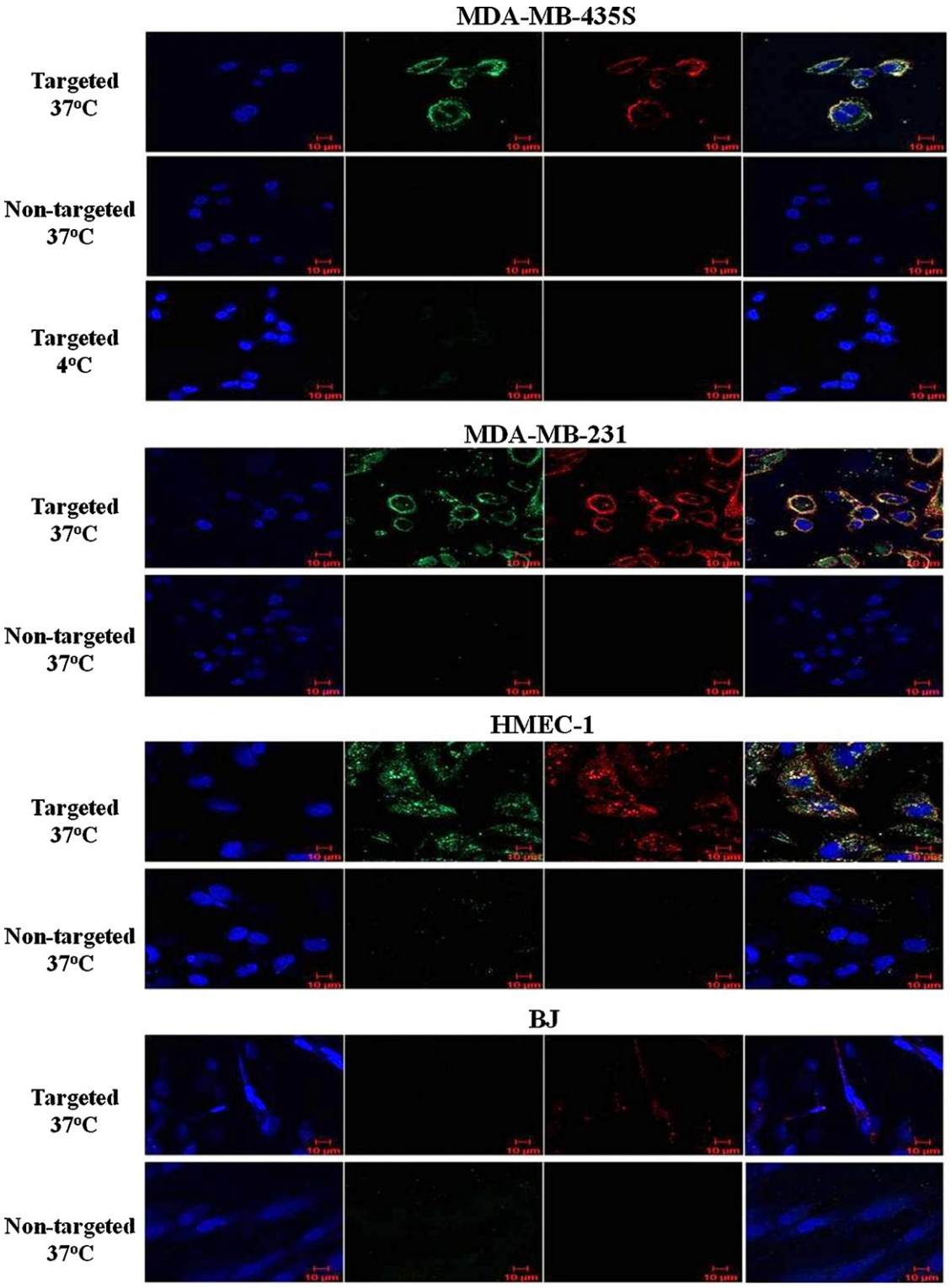

Fig. 2. Cellular association of F3-targeted and non-targeted liposomes with human cancer cell lines, endothelial cells and human fibroblasts, analyzed by confocal microscopy. MDA-MB-435S and MDA-MB-231 cancer cells, human microvascular endothelial cells (HMEC-1) or human non-cancer BJ fibroblasts (2.5×10^5) were incubated with rhodamine-labeled (red) F3-targeted and non-targeted liposomes, encapsulating FITC-labeled siRNA (green), at 0.2 mM of total lipid, during 1 h at 4 or 37 °C. The nucleus was stained with DAPI (blue). Cells were fixed with 4% paraformaldehyde, mounted in mowiol and visualized in a point scanning confocal microscope. (For interpretation of the references to color in this figure legend, the reader is referred to the web version of the article.)

incorporating 4 mol% PEG (data not shown). These results were likely related with the lower extent of liposomal uptake by the MDA-MB-231, relative to the MDA-MB-435.

In all the experiments performed, none of the tested formulations had a significant impact on cell viability (data not shown).

3.4. The inhibitory effect of PEG on the cellular association and intracellular trafficking

To better understand the effect of PEG on the transfection efficiency, we have first evaluated the extent of cellular association of

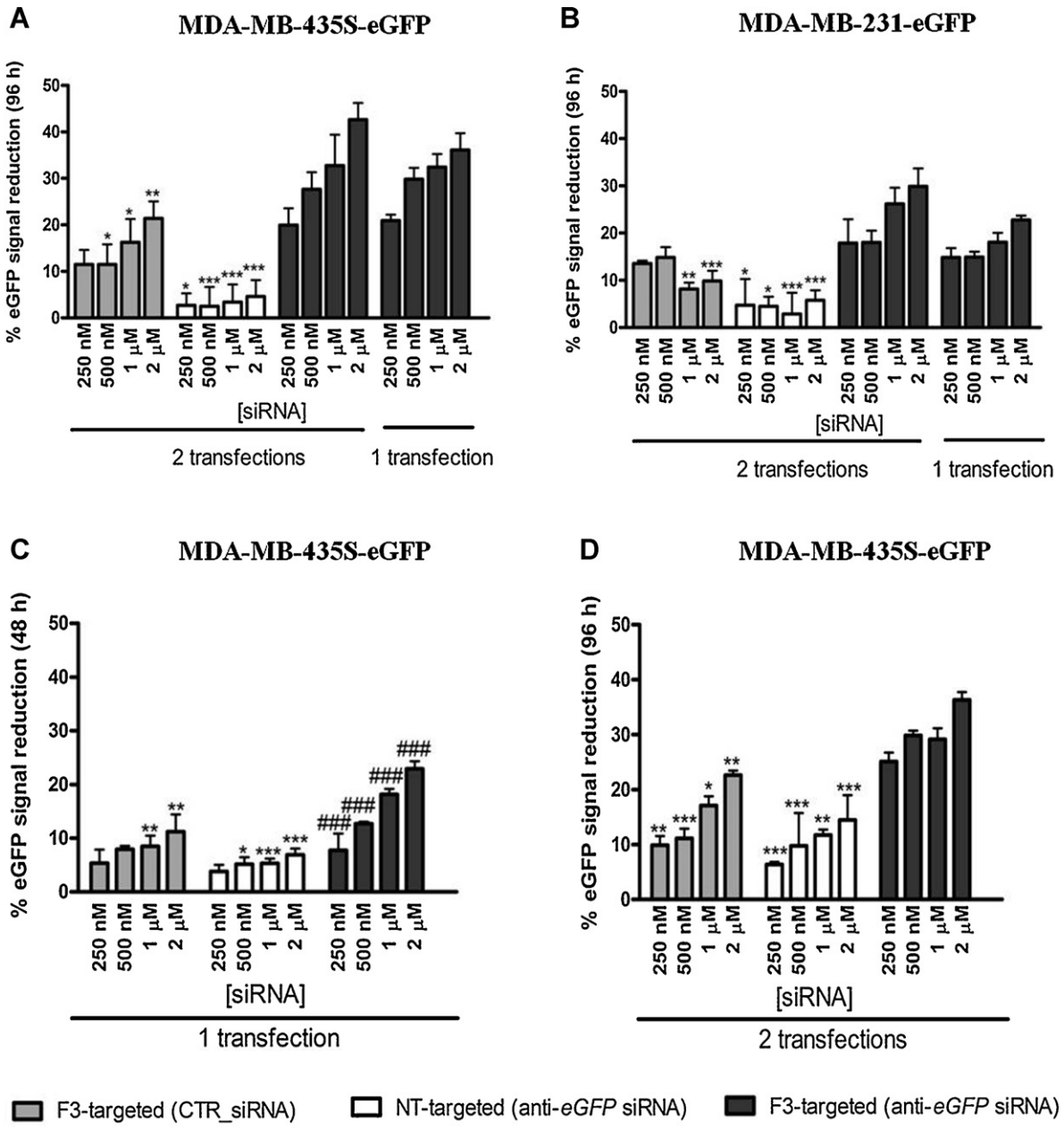

Fig. 3. Effect of the number of transfections, poly(ethylene glycol) content or treatment duration on eGFP levels. (A) MDA-MB-435S-eGFP and (B) MDA-MB-231-eGFP cell lines were transfected twice with different concentrations of anti-*eGFP* siRNA encapsulated in F3-targeted or non-targeted liposomes, incorporating 2 mol% of $CerC_{16}$-PEG_{2000}. A non-specific siRNA encapsulated in F3-targeted liposomes was included as control (CTR). Alternatively, only a single treatment was performed. EGFP levels were evaluated by flow cytometry 96 h after the beginning of the experiment. (C) EGFP levels were evaluated 48 h after one single treatment with liposomes composed of 2 mol% of $CerC_{16}$-PEG_{2000}. (D) MDA-MB-435-eGFP cells were transfected twice as in (A) but with liposomes formed with 4 mol% of $CerC_{16}$-PEG_{2000}. Bars are the mean ± SEM of 3 independent experiments. Two-way ANOVA analysis of variance with Bonferroni's post-test was used for multiple comparisons. *Asterik* symbols represented the significance level of the difference between the referenced formulations and the F3-targeted liposomes containing the anti-*eGFP* siRNA (***$p < 0.001$; **$p < 0.01$; *$p < 0.05$); *cardinal* symbols represented the significance level of the difference between eGFP levels at the referenced time point (###$p < 0.001$) when comparison was established between eGFP silencing at 48 h and 96 h.

F3-targeted liposomes incorporating 2 or 8 mol% of PEG. In fact, a slight decrease on the level of cellular association was observed for the formulation incorporating the highest amount of PEG (Fig. 4). However, these results did not explain *per se* the absence of protein downregulation associated with this formulation, as significant extent of association with the target cells was still achieved.

Being aware of how critical an efficient endosomal escape is for nucleic acids bioavailability and pharmacodynamics, the co-localization between FITC-labeled siRNA (green), delivered by each of those nanoparticles, with lysotracker red-labeled lysosomes (red) was assessed following an incubation period of 4 h. The strong yellow staining following incubation with targeted liposomes prepared with 8 mol% of PEG, suggested a higher extent of co-localization between siRNA and lysosomes (Fig. 5 A). In contrast, following delivery by liposomes with 2 mol% of PEG, a decrease on the intensity of the yellow staining suggested a decrease on the extent of co-localization (Fig. 5B). Overall, these results suggested that the high content of PEG strongly impair the siRNA endosomal escape, thus justifying the lack of activity of anti-*eGFP* siRNA delivered by F3-targeted liposomes incorporating 8 mol% of PEG.

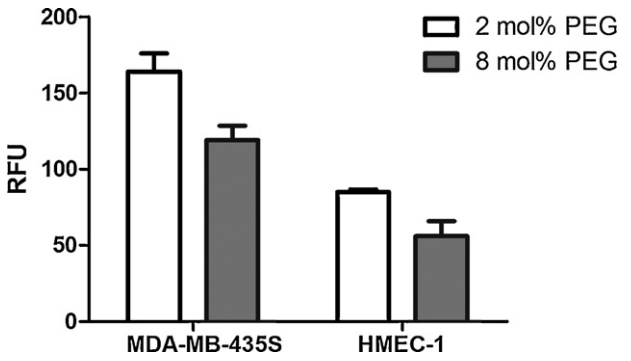

Fig. 4. Effect of PEG content on the extent of cellular association of F3-targeted liposomes by MDA-MB-435S cancer and HMEC-1 endothelial cells. Half-million cells were incubated with rhodamine-labeled F3-targeted liposomes incorporating 2 or 8 mol% of $CerC_{16}$-PEG_{2000}, at 0.2 mM of total lipid, for 1 h at 37 °C. After incubation, rhodamine signal was assessed by flow cytometry. Bars are the mean ± SD of 3 independent experiments. One-way ANOVA analysis of variance with Bonferroni's post-test was used for comparison between F3-targeted liposomes incorporating 2 and 8 mol% of PEG (ns: $p > 0.05$).

3.5. Evaluation of eGFP mRNA by qRT-PCR

Incubation of MDA-MB-435S-eGFP cells with F3-targeted liposomes containing the anti-*eGFP* siRNA led to an effective impact at the mRNA level, achieving a downregulation of 50% at 2 μM siRNA. This effect was dependent on the siRNA concentration (Fig. 6), as was also observed at the protein level by flow cytometry (Fig. 3). With non-targeted liposomes containing the anti-*eGFP* siRNA or F3-targeted liposomes containing a control siRNA, no significant downregulation of *eGFP* mRNA was observed (Fig. 6), evidencing both the molecular specificity of this approach and the importance of the intracellular delivery as well. Overall, these results pointed out the strong benefit of F3-targeted liposomes as a platform for the delivery of siRNA.

4. Discussion

As a therapeutic approach, gene silencing molecules, and particularly siRNA, provide solutions to the major drawbacks of traditional pharmaceutical drugs. The principal advantage over

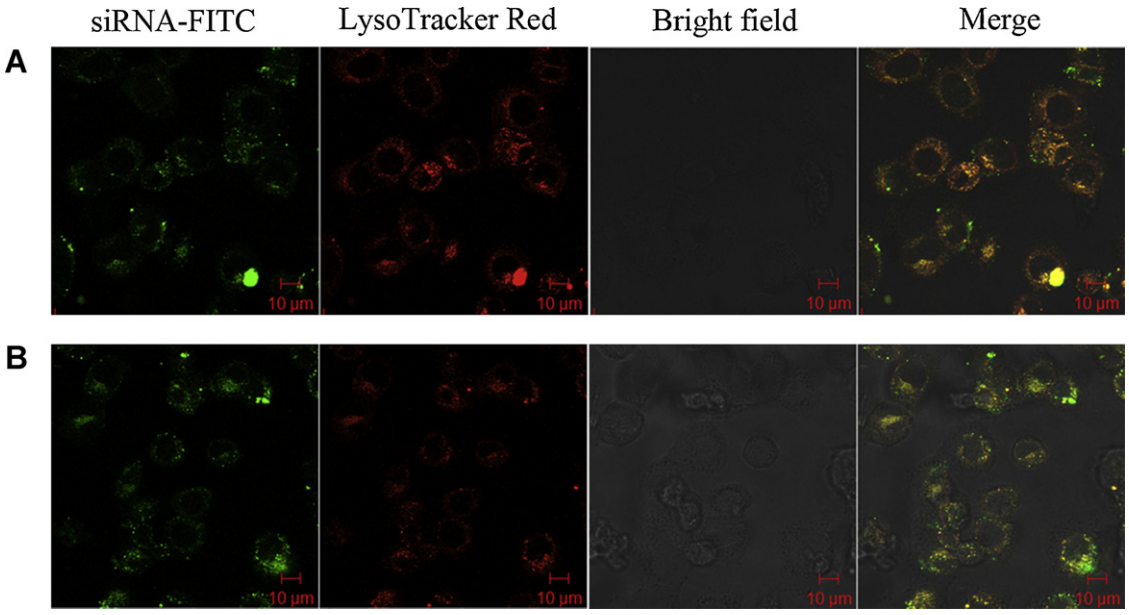

Fig. 5. Intracellular trafficking of siRNA encapsulated in F3-targeted liposomes. Cells were incubated with liposomes prepared either with (A) 8 or (B) 2 mol% of PEG, containing a FITC-labeled siRNA (green), during 4 h at 37 °C. Afterwards, lysosomes were labeled with LysoTracker Red (red) and live cells visualized in a point scanning confocal microscope. (For interpretation of the references to color in this figure legend, the reader is referred to the web version of the article.)

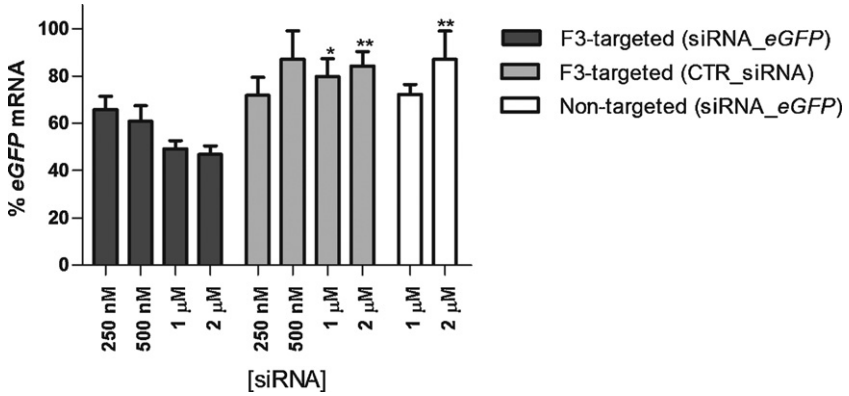

Fig. 6. Effect of anti-e*GFP* siRNA encapsulated in different liposomal formulations on the *eGFP* mRNA in MDA-MB-435S-eGFP cells. Cells were transfected at 0 and 48 h, with either anti-*eGFP* siRNA encapsulated in F3-targeted or non-targeted liposomes, containing 2 mol% of $CerC_{16}$-PEG_{2000}, or with the control siRNA encapsulated in the former. *EGFP* mRNA levels were assessed 24 h after the second transfection by qRT-PCR and in comparison with the mRNA levels of untreated cells. Bars are the mean ± SD of 3 independent experiments. Two-way ANOVA analysis of variance with Bonferroni's post-test was used for comparison between the referenced samples and F3-targeted liposomes containing the anti-*eGFP* siRNA (**$p < 0.01$, *$p < 0.05$).

small molecules and protein therapeutics are that all targets, including 'non-druggable' targets, can be inhibited by siRNA, which can be rapidly and rationally screened, designed and synthesized (Bumcrot et al., 2006).

Although siRNAs are one of the most promising class of RNAi mediators for therapeutic purposes, the clinical advancement of this strategy has been difficult to reach. This is particularly relevant when intravenous administration is envisaged as naked siRNAs are easily degraded by blood nucleases, rapidly eliminated by the kidneys and highly internalized by the reticuloendothelial system. Furthermore, even if the target cells are reached, the negative charge and hydrophilic nature of siRNAs strongly impair the cellular internalization (Castanotto and Rossi, 2009; Moreira et al., 2008). Such limitations emphasize the need for an efficient and safe system to modulate the siRNA pharmacokinetics and biodistribution.

In this respect, SALP (Maurer et al., 2001; Semple et al., 2001) and SNALP (Akinc et al., 2010; Geisbert et al., 2006; Judge et al., 2009; Morrissey et al., 2005; Zimmermann et al., 2006) fulfilled some of the requisites that should be present in a nanoparticle for intravenous administration of siRNA such as, high encapsulation efficiency, protection against nucleases, a small mean size, charge close to the neutrality and, prolonged blood circulation times. Nevertheless, those features are not enough to dictate an effective systemic siRNA delivery to distant sites of disease, like solid tumors localized in organs other than the liver. Actually, most of the studies involving sterically stabilized liposomes containing nucleic acids demonstrated that these particles naturally accumulate in the liver and spleen (Akinc et al., 2010; Geisbert et al., 2006; Judge et al., 2009; Kim et al., 2007; Morrissey et al., 2005; Zimmermann et al., 2006), being the accumulation into solid tumors still an enormous challenge. Despite this constraint, the aforementioned classes of liposomes represent an opportunity for further improvements on the targeted delivery to solid tumors upon covalently coupling of ligands targeting internalizing receptors. Antagonist G (Santos et al., 2010), transferrin (Mendonca et al., 2010) and folate (Yang et al., 2004) are examples of ligands which have been explored as targeting devices of nanoparticles of different nature, including liposomes similar to the ones herein described. However, these strategies aiming at targeting cancer cells have not increased the level of tumor accumulation, in comparison to their non-targeted counterpart, but rather the intracellular delivery of those liposomes that were able to cross the leaky tumor endothelium. In the work of Moreira et al. (Moreira et al., 2001a,b), tumor accumulation of antagonist G-targeted liposomes and the non-targeted counterpart was similar, despite the enhanced cellular internalization observed *in vitro* of the former. Moreover, Bartlett et al. (2007) also demonstrated that both non-targeted and transferrin-targeted siRNA polymer-based nanoparticles exhibited similar biodistribution and tumor accumulation. These results demonstrated that tumor accumulation of both cancer cell-targeted and non-targeted nanoparticles was highly dependent on the EPR effect rather than on the presence of a moiety targeting solely the cancer cells (Fang et al., 2011; Iyer et al., 2006; Li and Huang, 2008).

Since endothelial cells from tumor blood vessels are more accessible to any nanoparticle injected in the vascular compartment than cancer cells, and being aware of the importance of angiogenesis for the tumor growth and metastasis formation, several therapies targeting angiogenesis have been proposed as a complementary strategy to treat cancer (Abdollahi and Folkman, 2010; Hadj-Slimane et al., 2007). Therefore, a nanoparticle capable of guiding and concentrating a therapeutic siRNA into endothelial cells from angiogenic tumor blood vessels, in addition to cancer cells, is expected to result in improved tumor accumulation which ultimately will bring additional benefits in the treatment of cancer.

The identification of receptors overexpressed on the surface of cancer cells as well as on other cells that constitute the tumor microenvironment, gives rise to an avenue of different forms for therapeutic intervention in oncology. The nucleolin receptor is one of such target as it is overexpressed both on cancer cells and endothelial cells from the angiogenic blood vessels (Christian et al., 2003). Therefore, the F3 peptide, which has been demonstrated to be actively internalized by nucleolin, was chosen as the targeting moiety (Porkka et al., 2002).

Overall, the developed F3-targeted sterically stabilized liposomes were characterized by high nucleic acid encapsulation efficiency, ability to protect the encapsulated siRNA, a mean size around 200 nm, homogeneous particle size distribution and a surface charge close to neutrality, which are features that make these nanoparticles adequate for a siRNA systemic administration.

Moreover, cellular association studies demonstrated that the attachment of the F3 peptide to the liposomal surface resulted in a specific and high extent of internalization (more than 10-fold increase relative to the non-targeted counterpart) by both cancer and endothelial cells from angiogenic blood vessels, but not by non-cancer BJ cells (Figs. 2 and 3). However, it is important to point out that the improved uptake was not necessarily synonymous of an efficient gene silencing, as reported by Santos et al. (2010). In this work, the improved cellular association of antagonist G-targeted liposomes (similar to the ones used herein) and containing anti-*BCL2* siRNA, has not enabled any gene silencing in small cell lung cancer cell lines.

In contrast, our eGFP silencing studies demonstrated a significant reduction of eGFP expression in cells treated with anti-*eGFP* siRNA delivered by F3-targeted liposomes (composed of 2 mol% of PEG), both at the protein and mRNA levels, whereas no silencing was observed when cells were treated with the non-targeted counterpart. These results thus indicated that the presence of the F3-peptide brings an important advantage (Figs. 3 and 6).

With the purpose of obtaining liposomes more stable in respect to size, higher amounts of PEG (4 and 8 mol%) were tested. Despite the improvements achieved at the size level (average reduction of 50 nm), the resulting F3-targeted liposomes were unable to induce eGFP downregulation. Although PEG confers stability during the preparation process and favorable pharmacokinetics characteristics *in vivo* (Semple et al., 2001), Song et al. (2002) demonstrated that the incorporation of 5 mol% of Cer-PEG in cationic liposomes complexed with plasmid or antisense oligonucleotides (asODN), slightly impaired cellular internalization but severely inhibited the escape from endosomes of the internalized nucleic acid, thus compromising the transfection efficiency. After endocytosis, lipid mixing between liposomes and the endocytic membrane has to occur, leading to the disruption of the endosomal membrane and the subsequent release of the entrapped nucleic acid. However, the steric barrier imposed by PEG strongly inhibits this process. This effect is more prominent when PEG is attached to lipids with acyl chains longer than 14C, as the dissociation rate from the liposomal membrane is much slower. Similar results were also reported by others (Remaut et al., 2007; Zhang et al., 1999) as well as for nanocarriers based on polyethylenimine and cyclodextrin (Mishra et al., 2004). Despite this, as the present work aimed at developing liposomes that could mediate systemic delivery of siRNA to breast tumors, $CerC_{16}$-PEG_{2000} was deliberately used, since acyl chains longer than 14C were also associated with longer blood circulation times (Zhang et al., 1999).

Our results demonstrated a slight decrease on the rate of internalization of F3-targeted liposomes formed with 8 mol% of PEG (Fig. 4). However, the limiting step in respect to gene silencing was rather the inability to escape from the endosomes, as revealed by the observed co-localization between lysosomes and siRNA. These results have also indicated that the lack of activity of the anti-*BCL2*

siRNA delivered by antagonist G-targeted liposomes previously mentioned (Santos et al., 2010) was probably due to the presence of 10 mol% of $CerC_{16}$-PEG_{2000}.

Taken together, these results demonstrated that with formulations that are internalized through receptor-mediated endocytosis, as it happens with F3-targeted liposomes containing siRNA (Moura et al., 2011), a careful selection of the PEG-derivatized lipid content is required. This demand aims at guaranteeing liposomal size stability without compromising their ability to release the siRNA into the cell cytoplasm, where the RNA interference machinery is located.

Alternatively, it is interesting to notice that the obstacles imposed by the presence of high amounts of PEG, in this type of formulation, can be overcome through the selection of targeting ligands (such as transferrin) with fusogenic properties (da Cruz et al., 2001). In fact, Mendonca et al. (2010) have developed transferrin-targeted liposomes, similar to the liposomes described herein but formed with 8 mol% of PEG, which *in vitro* resulted in *BCR-ABL* silencing, at the mRNA and protein levels, in two leukemia cell lines. Moreover, Yang et al. (2004) have also achieved downregulation of EGFR upon treatment of KB cells with folate-targeted liposomes, composed with 10 mol% of PEG, indicating that folate, like transferrin, can also have some fusogenic properties at acidic pH. Nevertheless, and as discussed, such strategies targeting only cancer cells are not likely to significantly improved *in vivo* tumor accumulation.

Overall, the developed F3-targeted liposomes presented adequate features for intravenous administration of siRNA and led to a significant improvement in the internalization by both cancer and endothelial cells from angiogenic blood vessels, which was further correlated with an effective gene silencing. The present work represents an important contribution toward a nanoparticle with multi-targeting capabilities, both at the cellular and molecular level.

Acknowledgements

The authors would like to acknowledge Nuno Fonseca for his helpful discussion of this manuscript.

Lígia C. Gomes-da-Silva and Adriana O. Santos were students of the international PhD program on Biomedicine and Experimental Biology from the Center for Neurosciences and Cell Biology and recipients of fellowship from the Portuguese Foundation for Science and Technology (FCT) (ref.: SFRH/BD/33184/2007 and SFRH/BD/11817/2003, respectively). The work was supported by the Portugal-Spain capacitation program in Nanoscience and Nanotechnology (ref.: NANO/NMed-AT/0042/2007).

References

Abdollahi, A., Folkman, J., 2010. Evading tumor evasion: current concepts and perspectives of anti-angiogenic cancer therapy. Drug Resist. Updat. 13, 16–28.

Akinc, A., Querbes, W., De, S., Qin, J., Frank-Kamenetsky, M., Jayaprakash, K.N., Jayaraman, M., Rajeev, K.G., Cantley, W.L., Dorkin, J.R., et al., 2010. Targeted delivery of RNAi therapeutics with endogenous and exogenous ligand-based mechanisms. Mol. Ther. 18, 1357–1364.

Allen, T.M., Hansen, C., 1991. Pharmacokinetics of stealth versus conventional liposomes: effect of dose. Biochim. Biophys. Acta 1068, 133–141.

Allen, T.M., Hansen, C., Martin, F., Redemann, C., Yau-Young, A., 1991. Liposomes containing synthetic lipid derivatives of poly(ethylene glycol) show prolonged circulation half-lives in vivo. Biochim. Biophys. Acta 1066, 29–36.

Bartlett, D.W., Su, H., Hildebrandt, I.J., Weber, W.A., Davis, M.E., 2007. Impact of tumor-specific targeting on the biodistribution and efficacy of siRNA nanoparticles measured by multimodality in vivo imaging. Proc. Natl. Acad. Sci. U.S.A. 104, 15549–15554.

Bumcrot, D., Manoharan, M., Koteliansky, V., Sah, D.W., 2006. RNAi therapeutics: a potential new class of pharmaceutical drugs. Nat. Chem. Biol. 2, 711–719.

Castanotto, D., Rossi, J.J., 2009. The promises and pitfalls of RNA-interference-based therapeutics. Nature 457, 426–433.

Christian, S., Pilch, J., Akerman, M.E., Porkka, K., Laakkonen, P., Ruoslahti, E., 2003. Nucleolin expressed at the cell surface is a marker of endothelial cells in angiogenic blood vessels. J. Cell Biol. 163, 871–878.

da Cruz, M.T., Simoes, S., Pires, P.P., Nir, S., de Lima, M.C., 2001. Kinetic analysis of the initial steps involved in lipoplex–cell interactions: effect of various factors that influence transfection activity. Biochim. Biophys. Acta 1510, 136–151.

Di Paolo, D., Ambrogio, C., Pastorino, F., Brignole, C., Martinengo, C., Carosio, R., Loi, M., Pagnan, G., Emionite, L., Cilli, M., et al., 2011. Selective Therapeutic targeting of the anaplastic lymphoma kinase with liposomal siRNA induces apoptosis and inhibits angiogenesis in neuroblastoma. Mol. Ther. 19, 2201–2212.

Elbashir, S.M., Harborth, J., Lendeckel, W., Yalcin, A., Weber, K., Tuschl, T., 2001a. Duplexes of 21-nucleotide RNAs mediate RNA interference in cultured mammalian cells. Nature 411, 494–498.

Elbashir, S.M., Lendeckel, W., Tuschl, T., 2001b. RNA interference is mediated by 21- and 22-nucleotide RNAs. Genes Dev. 15, 188–200.

Fang, J., Nakamura, H., Maeda, H., 2011. The EPR effect: unique features of tumor blood vessels for drug delivery, factors involved, and limitations and augmentation of the effect. Adv. Drug Deliv. Rev. 63, 136–151.

Fire, A., Xu, S., Montgomery, M.K., Kostas, S.A., Driver, S.E., Mello, C.C., 1998. Potent and specific genetic interference by double-stranded RNA in *Caenorhabditis elegans*. Nature 391, 806–811.

Geisbert, T.W., Hensley, L.E., Kagan, E., Yu, E.Z., Geisbert, J.B., Daddario-DiCaprio, K., Fritz, E.A., Jahrling, P.B., McClintock, K., Phelps, J.R., et al., 2006. Postexposure protection of guinea pigs against a lethal ebola virus challenge is conferred by RNA interference. J. Infect. Dis. 193, 1650–1657.

Hadj-Slimane, R., Lepelletier, Y., Lopez, N., Garbay, C., Raynaud, F., 2007. Short interfering RNA (siRNA), a novel therapeutic tool acting on angiogenesis. Biochimie 89, 1234–1244.

Hanahan, D., Weinberg, R.A., 2011. Hallmarks of cancer: the next generation. Cell 144, 646–674.

Hutvagner, G., Zamore, P.D., 2002. A microRNA in a multiple-turnover RNAi enzyme complex. Science 297, 2056–2060.

Ishida, T., Iden, D.L., Allen, T.M., 1999. A combinatorial approach to producing sterically stabilized (Stealth) immunoliposomal drugs. FEBS Lett. 460, 129–133.

Iyer, A.K., Khaled, G., Fang, J., Maeda, H., 2006. Exploiting the enhanced permeability and retention effect for tumor targeting. Drug Discov. Today 11, 812–818.

Jemal, A., Bray, F., Center, M.M., Ferlay, J., Ward, E., Forman, D., 2011. Global cancer statistics. CA Cancer J. Clin. 61, 69–90.

Judge, A.D., Robbins, M., Tavakoli, I., Levi, J., Hu, L., Fronda, A., Ambegia, E., McClintock, K., MacLachlan, I., 2009. Confirming the RNAi-mediated mechanism of action of siRNA-based cancer therapeutics in mice. J. Clin. Invest. 119, 661–673.

Kim, S.I., Shin, D., Choi, T.H., Lee, J.C., Cheon, G.J., Kim, K.Y., Park, M., Kim, M., 2007. Systemic and specific delivery of small interfering RNAs to the liver mediated by apolipoprotein A–I. Mol. Ther. 15, 1145–1152.

Li, S.D., Huang, L., 2008. Pharmacokinetics and biodistribution of nanoparticles. Mol. Pharmacol. 5, 496–504.

Li, X., Zhao, X., Fang, Y., Jiang, X., Duong, T., Fan, C., Huang, C.C., Kain, S.R., 1998. Generation of destabilized green fluorescent protein as a transcription reporter. J. Biol. Chem. 273, 34970–34975.

Marchio, S., Lahdenranta, J., Schlingemann, R.O., Valdembri, D., Wesseling, P., Arap, M.A., Hajitou, A., Ozawa, M.G., Trepel, M., Giordano, R.J., et al., 2004. Aminopeptidase A is a functional target in angiogenic blood vessels. Cancer Cell 5, 151–162.

Maurer, N., Wong, K.F., Stark, H., Louie, L., McIntosh, D., Wong, T., Scherrer, P., Semple, S.C., Cullis, P.R., 2001. Spontaneous entrapment of polynucleotides upon electrostatic interaction with ethanol-destabilized cationic liposomes. Biophys. J. 80, 2310–2326.

Mendonca, L.S., Firmino, F., Moreira, J.N., Pedroso de Lima, M.C., Simoes, S., 2010. Transferrin receptor-targeted liposomes encapsulating anti-BCR-ABL siRNA or asODN for chronic myeloid leukemia treatment. Bioconjug. Chem. 21, 157–168.

Mishra, S., Webster, P., Davis, M.E., 2004. PEGylation significantly affects cellular uptake and intracellular trafficking of non-viral gene delivery particles. Eur. J. Cell Biol. 83, 97–111.

Moreira, J.N., Gaspar, R., Allen, T.M., 2001a. Targeting Stealth liposomes in a murine model of human small cell lung cancer. Biochim. Biophys. Acta 1515, 167–176.

Moreira, J.N., Hansen, C.B., Gaspar, R., Allen, T.M., 2001b. A growth factor antagonist as a targeting agent for sterically stabilized liposomes in human small cell lung cancer. Biochim. Biophys. Acta 1514, 303–317.

Moreira, J.N., Ishida, T., Gaspar, R., Allen, T.M., 2002. Use of the post-insertion technique to insert peptide ligands into pre-formed stealth liposomes with retention of binding activity and cytotoxicity. Pharm. Res. 19, 265–269.

Moreira, J.N., Santos, A., Moura, V., Pedroso de Lima, M.C., Simoes, S., 2008. Non-viral lipid-based nanoparticles for targeted cancer systemic gene silencing. J. Nanosci. Nanotechnol. 8, 2187–2204.

Morrissey, D.V., Lockridge, J.A., Shaw, L., Blanchard, K., Jensen, K., Breen, W., Hartsough, K., Machemer, L., Radka, S., Jadhav, V., et al., 2005. Potent and persistent in vivo anti-HBV activity of chemically modified siRNAs. Nat. Biotechnol. 23, 1002–1007.

Moura, V., Lacerda, M., Figueiredo, P., Corvo, M.L., Cruz, M.E., Soares, R., de Lima, M.C., Simoes, S., Moreira, J.N., 2011. Targeted and intracellular triggered delivery of therapeutics to cancer cells and the tumor microenvironment: impact on the treatment of breast cancer. Breast Cancer Res. Treat.

Papahadjopoulos, D., Allen, T.M., Gabizon, A., Mayhew, E., Matthay, K., Huang, S.K., Lee, K.D., Woodle, M.C., Lasic, D.D., Redemann, C., et al., 1991. Sterically stabilized liposomes: improvements in pharmacokinetics and antitumor therapeutic efficacy. Proc. Natl. Acad. Sci. U.S.A. 88, 11460–11464.

Porkka, K., Laakkonen, P., Hoffman, J.A., Bernasconi, M., Ruoslahti, E., 2002. A fragment of the HMGN2 protein homes to the nuclei of tumor cells and tumor endothelial cells in vivo. Proc. Natl. Acad. Sci. U.S.A. 99, 7444–7449.

Remaut, K., Lucas, B., Braeckmans, K., Demeester, J., De Smedt, S.C., 2007. Pegylation of liposomes favours the endosomal degradation of the delivered phosphodiester oligonucleotides. J. Control. Release 117, 256–266.

Santos, A.O., da Silva, L.C., Bimbo, L.M., de Lima, M.C., Simoes, S., Moreira, J.N., 2010. Design of peptide-targeted liposomes containing nucleic acids. Biochim. Biophys. Acta 1798, 433–441.

Semple, S.C., Klimuk, S.K., Harasym, T.O., Dos Santos, N., Ansell, S.M., Wong, K.F., Maurer, N., Stark, H., Cullis, P.R., Hope, M.J., et al., 2001. Efficient encapsulation of antisense oligonucleotides in lipid vesicles using ionizable aminolipids: formation of novel small multilamellar vesicle structures. Biochim. Biophys. Acta 1510, 152–166.

Song, L.Y., Ahkong, Q.F., Rong, Q., Wang, Z., Ansell, S., Hope, M.J., Mui, B., 2002. Characterization of the inhibitory effect of PEG–lipid conjugates on the intracellular delivery of plasmid and antisense DNA mediated by cationic lipid liposomes. Biochim. Biophys. Acta 1558, 1–13.

Torchilin, V.P., 2010. Passive and active drug targeting: drug delivery to tumors as an example. Handb. Exp. Pharmacol., 3–53.

Yang, L., Li, J., Zhou, W., Yuan, X., Li, S., 2004. Targeted delivery of antisense oligodeoxynucleotides to folate receptor-overexpressing tumor cells. J. Control. Release 95, 321–331.

Zhang, Y.P., Sekirov, L., Saravolac, E.G., Wheeler, J.J., Tardi, P., Clow, K., Leng, E., Sun, R., Cullis, P.R., Scherrer, P., 1999. Stabilized plasmid-lipid particles for regional gene therapy: formulation and transfection properties. Gene Ther. 6, 1438–1447.

Zimmermann, T.S., Lee, A.C., Akinc, A., Bramlage, B., Bumcrot, D., Fedoruk, M.N., Harborth, J., Heyes, J.A., Jeffs, L.B., John, M., et al., 2006. RNAi-mediated gene silencing in non-human primates. Nature 441, 111–114.